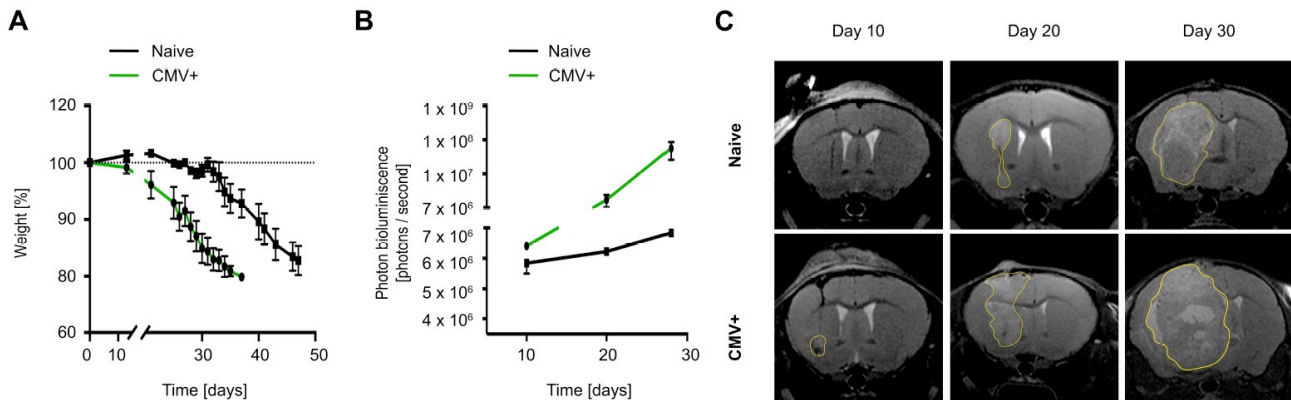
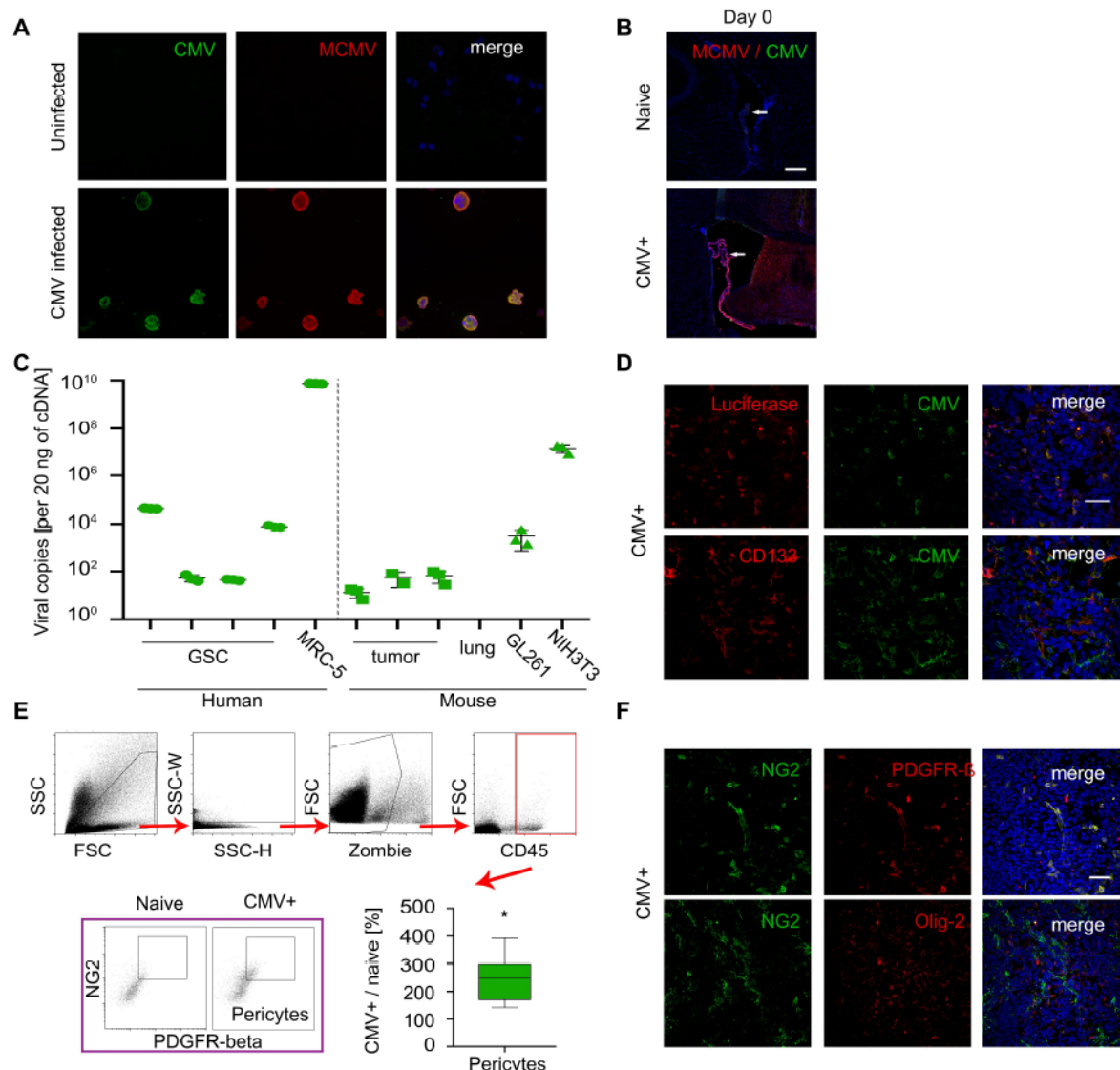


Supplementary Figures

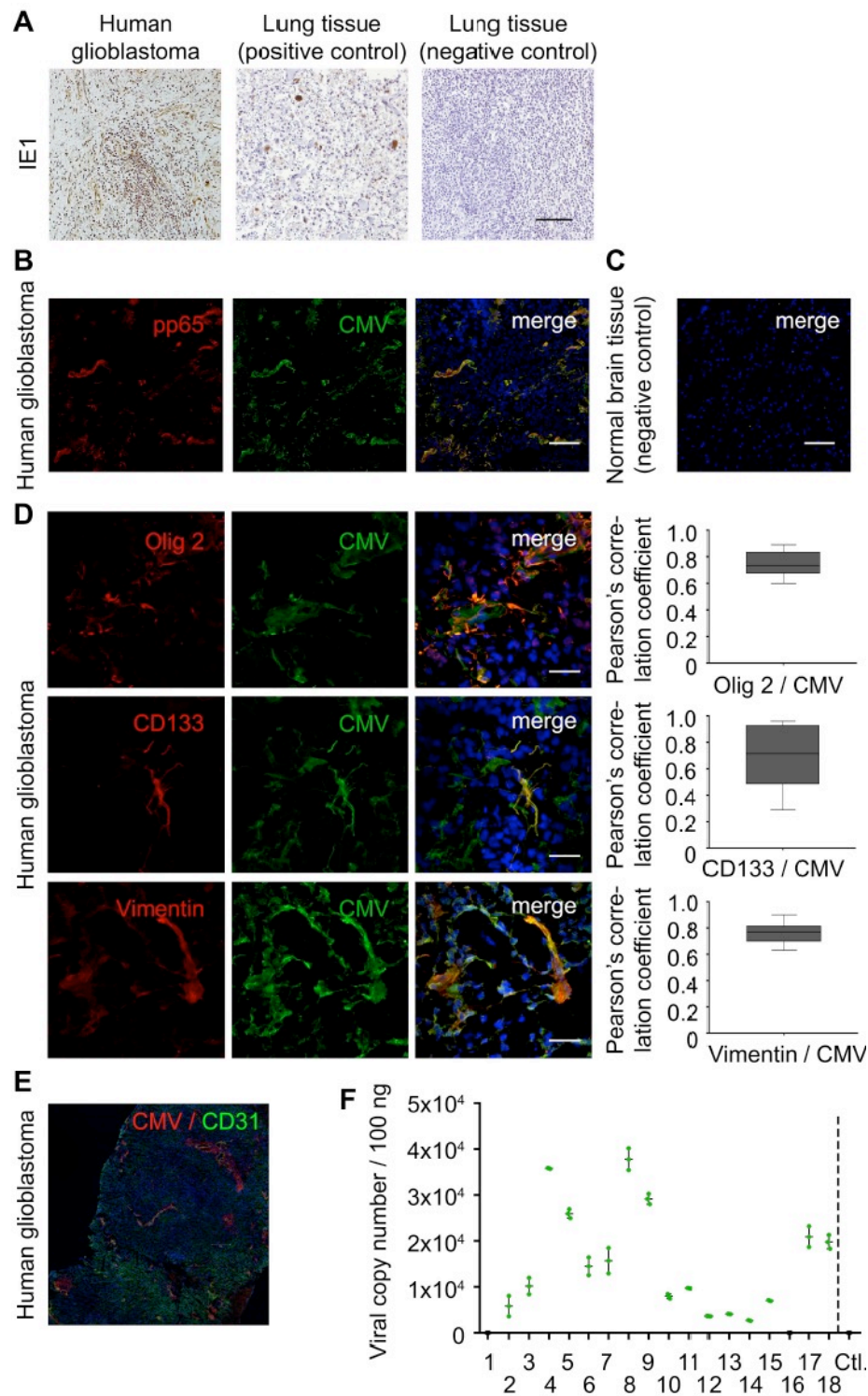


Supplementary Figure 1. Accelerated GBM growth in MCMV-infected mice a, Weight curve of mice intracranially implanted with GL261Luc2 cells. Data is shown as mean \pm SD values. **b,** BLI of tumors implanted in uninfected and MCMV+ mice 10, 20 and 30 days after tumor cell injection. Data is shown as mean \pm SD values **c,** Time-matched T2-weighted MRI depicting tumor growth over time. Uninfected controls are shown in the upper panels, and MCMV+ animals in the lower panels at Days 10, 20 and 30 post tumor cell injection. The tumor boundary is indicated by the yellow line.



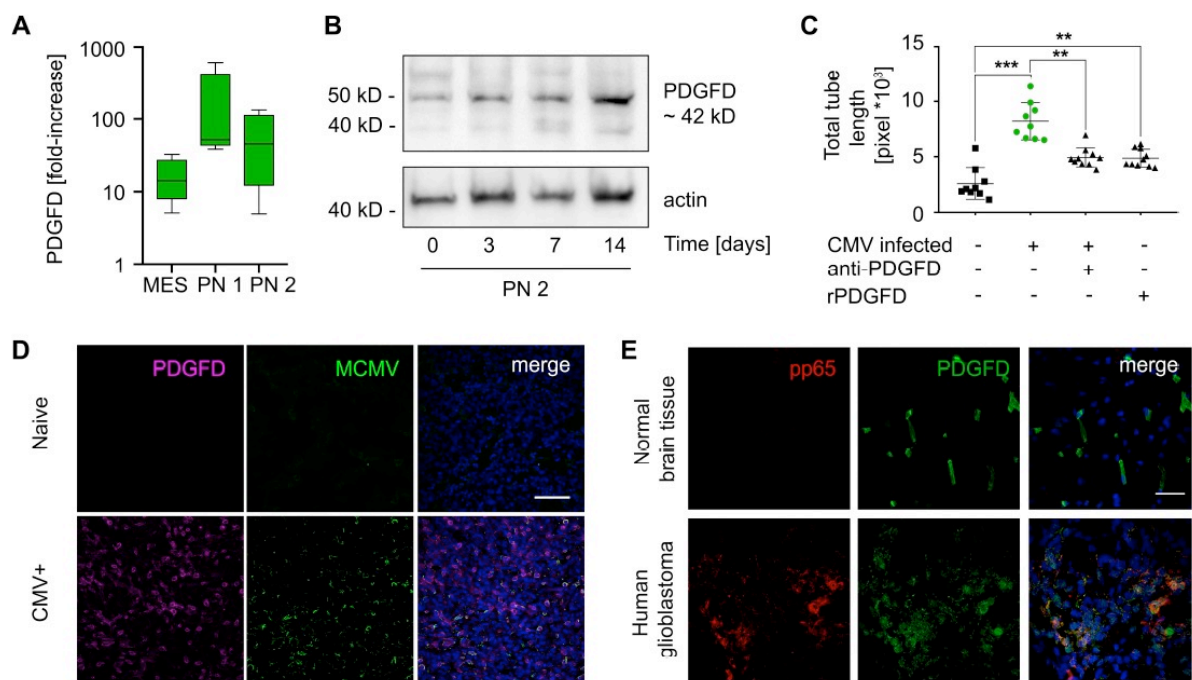
Supplementary Figure 2. MCMV detection and increased pericyte numbers in GL261Luc2 tumors *in vivo*. **a**, CMV (green) and MCMV (red) staining in MCMV infected GL261 cells *in vitro* 48 hours post-infection. **b**, CMV (green) and MCMV (red) Immunofluorescence in MCMV+ mice aged 14 weeks, without tumor implantation. MCMV is detected in the ventricular wall, choroid plexus and subventricular zone (arrow) in brains of MCMV+ mice prior to tumor injection (scale bar = 200 μ m). **c**, Luciferase (red), CD133 (red) and MCMV (green), nuclei (blue) Immunofluorescence staining with in brain sections taken from animals at the endpoint of survival studies (scale bar = 50 μ m). Pearson's rank co-localization (mean

\pm SD) from $n = 3$ tumor specimens. Error bars indicate SD. **d**, Quantitative RT-PCR analysis of HCMV IE1 in G44 GSCs, and in MRC5 fibroblasts, and MCMV in tumor from MCMV+ mice, MCMV+ tumor-bearing mouse lung ($n+3$) and in MCMV infected GL261 cells **e**, Flow cytometric quantification of tumour infiltrating pericytes. Dot plots represent NG2/PDGFR- β double-positive cells within the ipsilateral hemisphere in MCMV+ ($n = 3$) and naïve mice ($n = 3$). In the graphical representation the box extends from the 25th to 75th percentile, and the median is indicated by a horizontal line. The whiskers represent the maximum and minimum values.* $P < 0.05$ (two-way ANOVA). **f**, Upper panel shows anti-PDGFR- β (red) and NG2 (green) immunostaining confirming presence of pericytes in GBMs growing in MCMV+. The lower panel shows Olig2 (red) and NG2 (green) co-staining. DAPI stained nuclei are shown in blue (scale bar = 50 μ m).



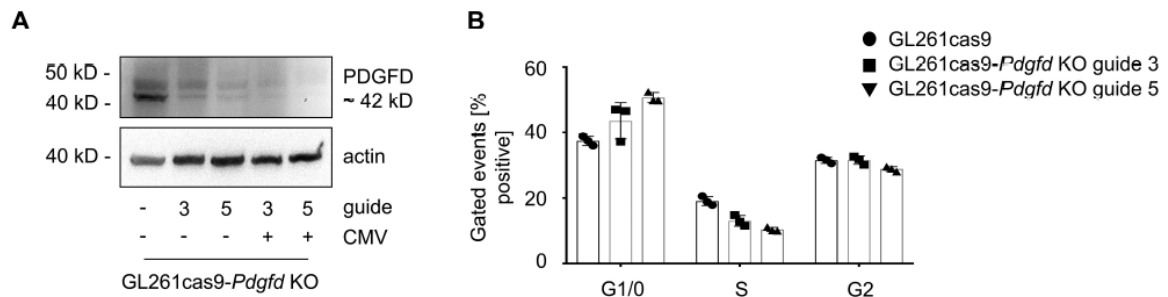
Supplementary Figure 3. HCMV is detectable in human GBM tissue and associates with the perivascular niche. **a**, IE-1 immunohistochemical staining in human GBM and HCMV positive lung control tissue. (scale bar = 50 μ m) **b**, CMV (green) and pp65 (red) immunofluorescence in human GBM specimens and **c**, cortical tissue (control) DAPI stained nuclei are shown in blue. **d**, CMV (green), Olig2

(red), anti-CD133 (red) and vimentin (red), and nuclei (blue) immunofluorescence staining (scale bar = 50μm). In graphical representations the box extends from the 25th to 75th percentile, and the median is indicated by a horizontal line. The whiskers represent the maximum and minimum values. **e**, HCMV (red) and CD31 (green) staining in a representative human GBM specimen. **f**, Quantitative RT-PCR analysis of HCMV IE1 mRNA levels in human GBM specimens.



Supplementary Figure 4. PDGF-D regulates the CMV-induced vascular phenotype and plays a critical role in GL261 tumor growth. **a**, RT-PCR analysis of PDGF-D mRNA in multiple GSCs three days after HCMV infection. The box extends from the 25th to 75th percentile, and the median is indicated by a horizontal line. The whiskers represent the maximum and minimum values.. **b**, Western blot analysis of PDGF-D in proneural GSCs at days 0, 3, 7 and 14 post HCMV infection. **c**, HBMEC tube formation on matrigel performed using conditioned media from HCMV-infected human GSCs four days post-infection as well as uninfected control media, in the presence and absence of recombinant human PDGF-D and anti-PDGF-D neutralizing antibodies. Data analysis is presented as mean \pm SD ** P < 0.01, *** P

< 0.001 , Holm-Šídák test. **d**, pp65 (green) and mouse PDGF-D (magenta) immunostaining in brain sections taken from animals at the endpoint of survival studies. DAPI stained nuclei are shown in blue (scale bar = 50 μ m). **e**, pp65 (green), PDGF-D (magenta) and nuclei (blue) immunofluorescence in GBM sections (scale bar = 50 μ m). Panels from this figure are also shown in Fig. 5G.



Supplementary Figure 5. Effect of *Pdgfd* knockdown on cell cycle parameters in GL261cas9 cells. **a**, Western blot analysis of PDGF-D in uninfected and MCMV-infected GL261*Pdgfd*KO cells (guides 3 and 5). **b**, Cell cycle distribution of GL261*Pdgfd*KO (guides 3 and 5) cells was measured (uninfected vs. MCMV-infected (MOI 1)). Data are represented as mean \pm SD. * $P < 0.05$, ** $P < 0.01$, *** $P < 0.001$, two-way ANOVA.

Supplementary Table 1. Proangiogenic genes identified in CMV infected GSCs from RNA-Seq data.

Gene ID	Gene name	Log2 fold change CMV/normal	Adjusted P Value	Major Functions	Function in glioblastoma
BMP4	Bone morphogenetic protein 4	4.588902	8.37E-20	Development	Pro-differentiation (33)
CCL2	C-C motif chemokine ligand 2 (MCP1)	7.640191	2.26E-94	Monocyte chemoattraction	Treg and MDSC recruitment (34)
CXCL8	C-X-C motif chemokine ligand 8 (Interleukin 8)	5.700278	3.00E-46	Pro-inflammatory	Pro-angiogenic (35)
LIF	Leukemia Inhibitory Factor	3.243461	1.64E-169	Pleiotropic cytokine	Promotes Glioma stem cell renewal (36)
PDGFD	Platelet-derived growth factor δ	2.753318	0.001808	Percyte recruitment	NOT STUDIED
WNT4	wingless-type MMTV integration site family, member 4	3.087092	0.000339	Development	CNS specific angiogenesis (37)

We profiled gene expression in G44 GSCs after CMV infection. To identify genes potentially involved with the proangiogenic phenotype, we curated a list for proangiogenic soluble factors from genes intersecting between GO: 1901342 (regulation of vascular development) and M5883 (BIOCARTA MsigDB, genes encoding secreted soluble factors). This list was then intersected with significantly upregulated genes from RNA-Seq leading to a final number of 6 genes with known proangiogenic functions as shown.

Supplementary Table 2

Primer sequences used in the study

Species/Gene	Fwd/Rev	Sequence
Mouse		
		Orientation (5'/3')
Ppia	Fwd	CAAACACAAACGGTTCCCAG
Ppia	Rev	TTCACCTTCCCAAAGACCAC
PDGFD	Fwd	CCAAGGAACCTGCTTCTGAC
PDGFD	Rev	CTTGGAGGGATCTCCTTGTG
mIE1	Fwd	AGCCACCAACATTGACCACGCAC
mIE1	Rev	GCCCCAACCAGGACACACAACCTC
Human		
18s	Fwd	GTAACCCGTTGAACCCCATT
18s	Rev	CCATCCAATCGGTAGTAGCG
PDGFD	Fwd	GAACAGCTACCCCAGGAACC
PDGFD	Rev	CTTGTGTCCACACCATCGTC